ORGANIC CHEMISTRY FRONTIERS

RESEARCH ARTICLE

View Article Online
View Journal | View Issue

Cite this: *Org. Chem. Front.*, 2024, **11**, 4470

Stereoselective strain-release Ferrier rearrangement: the dual role of catalysts†

Huajun Zhang,‡ Aoxin Guo,‡ Han Ding, ‡ Yuan Xu, Yuhan Zhang, Dan Yang and Xue-Wei Liu *

Received 30th April 2024,
Accepted 19th June 2024

DOI: 10.1039/d4qo00410h

rsc.li/frontiers-organic

Herein, we report an efficient, stereoselective synthesis of 2,3-unsaturated glycosides under mild conditions through a novel Ferrier rearrangement of reasonably designed glycal donors with C3-position *ortho*-2,2-dimethoxycarbonycyclopropylbenzoyl (CCBz), facilitated by user-friendly, eco- and environmental-friendly $Cu(OTf)_2$ or $Fe(OTf)_3$. The newly devised rearrangement tactic is highly α-stereoselective and applies to a broad scope of nucleophile acceptors, enabling the construction of 2,3-unsaturated *O*-, *S*-, *N*-, and *C*-glycosides, with exceptional yields and stereoselectivities. DFT calculations were conducted to elucidate the reaction mechanism, unveiling the dual role of the metal catalysts in activating the glycal donor through promoting ring-opening of the intramolecularly incorporated donor–acceptor cyclopropane (DAC) of CCBz and directing the following α-face-preferential nucleophilic attack of the incoming acceptor mediated by H-bond interactions.

Introduction

Carbohydrates feature essential roles in manifold physiological processes, including cellular respiration, cell–cell contact and adhesion, modulating transcription and sophisticated cascades, inflammation, and post-translational modifications.[1] Among the diverse carbohydrate structures, 2,3-unsaturated glycosides stand out for their significant pharmacological properties and retrofittable potential in organic synthesis (Fig. 1A). The naturally occurring unsaturated sugar derivative blasticidin S, fortuitously discovered in the 1950s,[2] prevents rice blast disease. Synthetic compounds containing 2,3-unsaturated sugars also show potent bioactivities. 7-*O*-(4,6-di-*O*-acetyl-hex-2-enea-D-*erythro*-pyranosyl) genistein, a genistein derivative, suppresses tumor growth.[3,4] Stavudine, a synthetic L-nucleoside that has been approved as the fourth anti-HIV drug, inhibits the HIV reverse transcriptase with fewer adverse effects on bone marrow stem cells and mitochondrial DNA replication[5] than the predecessor AZT. Meanwhile, the 2,3-olefinic bond in a pyranose ring is amenable to facile functionalization at C2- and C3-positions *via* a variety of well-established reactions such as asymmetric dihydroxylation, amino hydroxylation, hydrogenation, and epoxidation, underscoring the wide applications of this type of scaffold in synthesizing diverse functionalized sugar structures.[6]

Glycals have long been exploited as synthons for chemical derivatizations to various sugar adducts and derivatives. The Ferrier I rearrangement of glycals proves to be a facile and efficient approach for creating 2,3-unsaturated pyranose scaffolds. In a classical Ferrier I rearrangement, glycal with a good leaving group (LG) at the C3-position, such as acetate, carbonate, or trichloroacetimidate, is first activated, then an allylic rearrangement on the pyranose ring occurs, accompanied by the dissociation of the C3-LG and the ensuing attack of a nucleophile at the anomeric position, affording the 2,3-unsaturated glycoside (Fig. 1B, a).[7] Many Ferrier rearrangement reactions under mild conditions with short reaction times consume stoichiometric amounts of Lewis acids as promoters, while other transformations are either promoted by Brønsted acids[8] or transition metal catalysts.[9,10] A Ferrier-type *O*-glycosylation through a radical pathway employing single-electron transfer reagents[11] and chemical oxidants like 2,3-dichloro-5,6-dicyano-1,4-benzoquinone (DDQ) or ceric ammonium nitrate (CAN) has also been reported (Fig. 1B, c).[12] Recently, Nagaki and coworkers reported flash electrochemical and superacid-promoted pathways leading to nitrogen-containing 2,3-unsaturated *C*-aryl glycosides and *C*-alkyl glycosides respectively *via* short-lived intermediates (Fig. 1B, b).[13] Despite these advancements, current Ferrier reactions are often limited to narrow substrate scopes and poor-to-moderate α-selectivities during glycosidic linkage formation, which is influenced by multiple factors of the vinylogous anomeric effect (VAE)[14] that is affected by the orientation of the C4-sub-

School of Chemistry, Chemical Engineering and Biotechnology, 21 Nanyang Link, 637371 Singapore. E-mail: xuewei@ntu.edu.sg

†Electronic supplementary information (ESI) available. See DOI: https://doi.org/10.1039/d4qo00410h

‡These authors contributed equally to this work.

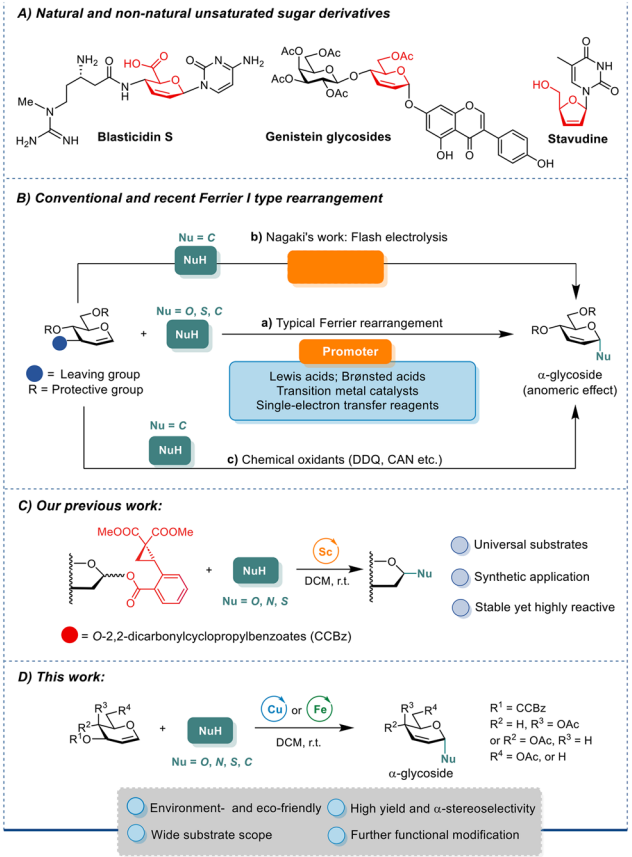

Fig. 1 Significance of and synthetic approaches to 2,3-unsaturated glycosides and our strategy.

stituent, 1,3-diaxial interactions, the substituents at C5,[15] as well as the solvent effect in most cases.[16,17]

Our group is long devoted to the development of novel glycosylation methodologies,[18] and we have developed a novel *ortho*-2,2-dimethoxycarbonylcyclopropylbenzoate (CCBz)[19] leaving group which can readily be activated by the $Sc(OTf)_3$ recently (Fig. 1C). The ring-strain release of intramolecular incorporated donor–acceptor cyclopropanes (DACs) in CCBz during LG dissociation efficiently drives glycosylation reactions with various *O*-, *S*-, and *N*-nucleophiles.[20] Drawing inspirations from the synthetic prowess of the CCBz LG, herein, we report the development of a novel Ferrier rearrangement for stereoselective construction of 2,3-unsaturated α-glycosides employing low-cost $Cu(OTf)_2$ or $Fe(OTf)_3$ catalysts under mild conditions by introducing CCBz to C3-position of glycal. Results from DFT simulations of the reaction pathways reveal that the α-stereoselectivity of the $Cu(OTf)_2$-catalyzed Ferrier rearrangement arises from the face-preferential directed nucleophilic attack mediated by the non-covalent interactions between metal-bound triflate and the incoming alcohol, denoting a dual-tasked $Cu(OTf)_2$ (Fig. 1D). Our approach provides facile, efficient, and stereoselective access to the synthetically valuable 2,3-unsaturated pyranose (pseudo-glycals) as chiral precursors for numerous further chemical transformations.

Results and discussion

We commenced our study by evaluating the feasibility of the proposed reaction and optimizing reaction conditions, using L-menthol **2a** as the model acceptor substrate. The results, detailed in Table 1, showed that employing glucal **1a** as the donor had an impressive 98% conversion but unsatisfactory stereoselectivity using $Sc(OTf)_3$ as the catalyst in dichloromethane (DCM, entry 1). Interestingly, significant improvements in stereoselectivities were observed employing $Cu(OTf)_2$ or $Fe(OTf)_3$, supplying the desired products in 98% yields with 10 : 1 α-selectivity (entries 2 and 3). Lowering the catalyst loading of $Fe(OTf)_3$ in the reaction system resulted in a drastic decrease in yield, while the stereoselectivity was not affected (entry 4). In contrast to $Fe(OTf)_3$, $FeCl_3$ produced minimal product conversion, probably due to its hygroscopic and deliquescent nature (entry 6). The ferrous salts with lower valence (+2) iron ions were ineffective for catalyzing the reaction (entries 5–7). Similarly, non-chelatable Lewis acids and Brønsted acids did not facilitate the reaction (entries 8 and 9). A screening of reaction solvents revealed that 1,2-dichloroethane (DCE) was also an efficient solvent (entries 10 and 11). However, utilizing Et_2O resulted in moderate yield and

Table 1 Reaction optimization

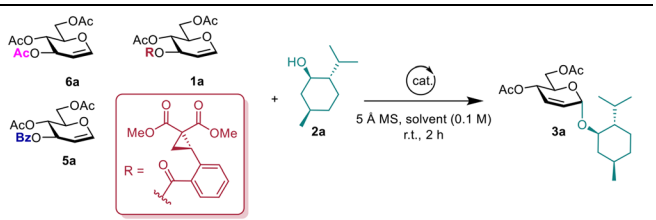

Entry	Donor	Catalyst	Solvent	Yield of **3a** %[b]	α : β[c]
1	**1a**	$Sc(OTf)_3$	DCM	98	4 : 1
2	**1a**	$Cu(OTf)_2$	DCM	98	10 : 1
3	**1a**	$Fe(OTf)_3$	DCM	98	10 : 1
4[d]	**1a**	$Fe(OTf)_3$	DCM	53	10 : 1
5	**1a**	$Fe(OTf)_2$	DCM[e]	N.R.[e]	N.D.[f]
6	**1a**	$FeCl_3$	DCM	6	—
7	**1a**	$FeCl_2$	DCM	N.R.	N.D.
8	**1a**	TMSOTf	DCM	N.R.	N.D.
9	**1a**	TfOH	DCM	N.R.	N.D.
10	**1a**	$Cu(OTf)_2$	DCE[f]	98	10 : 1
11	**1a**	$Fe(OTf)_3$	DCE	98	10 : 1
12	**1a**	$Cu(OTf)_2$	Et_2O	65	10 : 3
13	**1a**	$Fe(OTf)_3$	Toluene	12	10 : 1
14	**1a**	$Fe(OTf)_3$	ACN[g]	N.R.[h]	N.D.[i]
15	**5a**	$Cu(OTf)_2$	DCM	N.R.	N.D.
16	**5a**	$Fe(OTf)_3$	DCM	N.R.	N.D.
17	**6a**	$Cu(OTf)_2$	DCM	74%	3 : 1
18	**6a**	$Fe(OTf)_3$	DCM	69%	3 : 1

[a] Unless otherwise noted, all reactions were carried out with **1a** or **5a** (0.1 mmol, 1.0 equiv.), **2a** (1.2 equiv.), catalyst (0.1 equiv.) and 5 Å MS (50 mg) in corresponding solvent (1.0 mL, 0.1 M) under nitrogen atmosphere for 2 h. [b] Isolated yields. [c] The α : β ratios were determined by ^{1}H NMR analysis. [d] 0.05 equiv. of catalyst. [e] DCM = dichloromethane. [f] DCE = 1,2-dichloroethane. [g] ACN = acetonitrile. [h] N.R. = no reaction. [i] N.D. = not detected. [j] MS = molecular sieve.

stereoselectivity (entry 12), and this reaction failed to proceed in toluene and acetonitrile (ACN) at room temperature (entries 13 and 14). Subjecting the contrast donor 3-*O*-benzoyl-4,6-di-*O*-acetyl-glucal **5a** to the optimized conditions did not lead to the formation of the corresponding product. This result suggests that the catalyst's activation of the DAC site occurs through chelation with two carbonyl groups (entries 15 and 16).[21] Lastly, when tri-*O*-acetyl-D-glucal (**6a**) as a donor to the optimized conditions did not obtain the desired product **3a** in great yield and α-stereoselectivity (entries 17 and 18).

To explore the substrate scope of the $Cu(OTf)_2$- or $Fe(OTf)_3$-catalyzed Ferrier reaction, we subjected a library of structurally diverse acceptors (**2b–2u**) to the reaction with **1a** under the optimized reaction conditions, as depicted in Table 2. This set of acceptors included aliphatic alcohols with primary, secondary, and tertiary hydroxyl groups, sugar alcohols, phenol, and heteroatom nucleophiles. The results were encouraging, yielding corresponding 2,3-unsaturated glucosides in 56% to 98% yields. Notably, the reaction results were predominantly α selectivities (α : β = 3 : 1 to α only, determined by ^{1}H NMR analysis). Additionally, the strain-release glycosylation effectively promoted the reaction of **1a** with thioglycoside acceptors, producing unsaturated disaccharide thioglycosides (**3l** and **3k**). Interestingly, the typical aglycone transfer often seen with thioglycoside acceptors was not observed.[22] Although reactions with **2m** and **2o** took 12 hours to complete, acid-sensitive acetonides were well tolerated, forming **3m** and **3o** products. Under our mild reaction conditions, we selectively constructed the α-*O*-glycosidic bond with the C2–OH of mannoside **2p** and the C4–OH of rhamnoside **2n**. Notably, only $Cu(OTf)_2$ successfully promoted the Ferrier rearrangement of **2n**, while $Fe(OTf)_3$ resulted in a complex reaction mixture. A similar result was also observed when *para*-methoxyphenol **2d** was subjected to reaction with **1a** under the catalysis of $Fe(OTf)_3$, possibly due to the oxidation of the *para*-methoxyphenyl group by the oxidizing ferric ion. We further applied this methodology to the syntheses of complex and bioactive natural products and drugs. The α-*O*-glycosides building block was successfully installed onto the C3–OH of cholesterol **2g**, diosgenin **2h** and triterpene oleanolate **2i**, affording the respective glyconjugates **3g**, **3h** and **3i** in good yields and stereoselectivities (72% to 89%, α : β = 10 : 1 to 12 : 1). Additionally, the hormone pregnenolone (**2f**) and the antihyperlipidemic drug simvastatin (**2j**) were also compatible with our method, although longer reaction times were required.

Heteroatom glycosidic linkages, *i.e.*, which are glycosidic bonds where the anomeric oxygen in the hemiacetal sugars is replaced with a different atom, are widely found in a variety of important biological molecules, including glycoconjugates, glycopeptides,[23] glycosylamines,[24] glycolipids,[25] as well as in DNA, RNA, and coenzyme A.[26] To our delight, we confirmed that our Ferrier rearrangement applies to the synthesis of 2,3-

Table 2 Acceptors scope studies

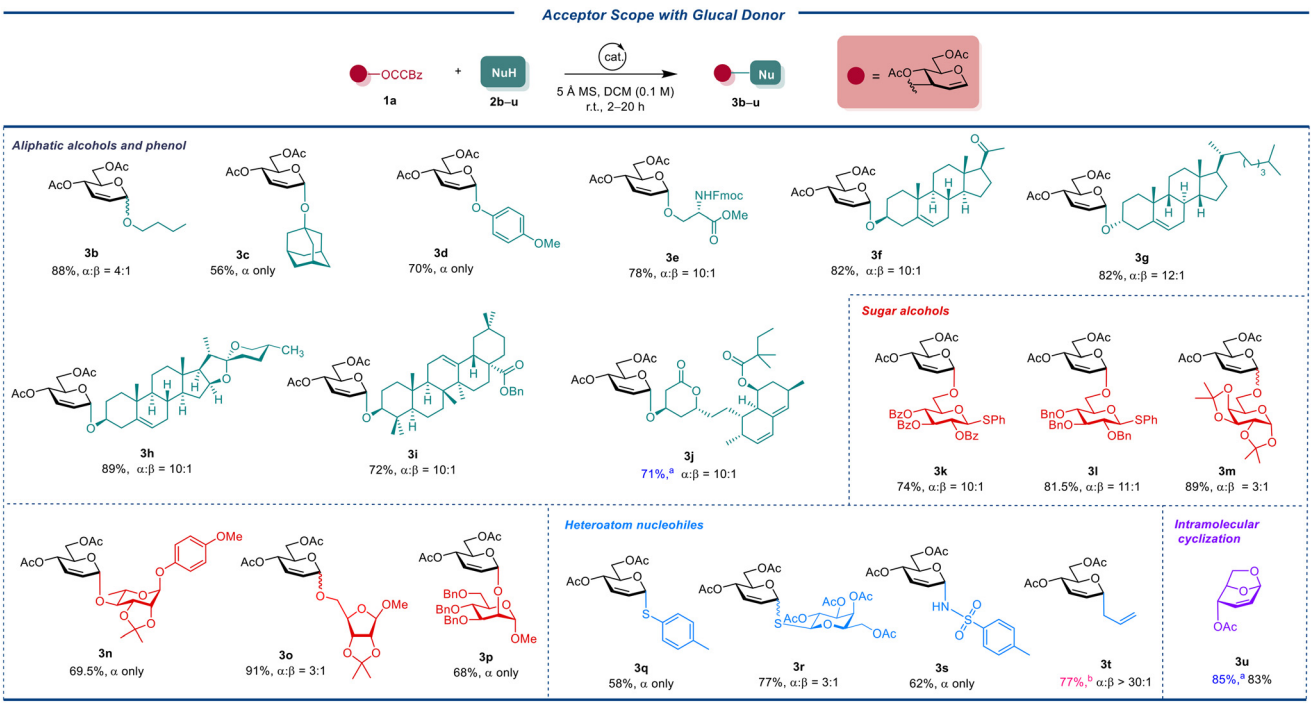

Conditions: unless otherwise noted, all reactions were carried out with **1a** (0.1 mmol, 1.0 equiv.), **2b–u** (1.2 equiv.), $Cu(OTf)_2$ (0.1 equiv.) and 5 Å MS (50 mg) in distilled DCM (1.0 mL, 0.1 M) under nitrogen atmosphere at the room temperature. [a] $Fe(OTf)_3$ (0.1 equiv.) and 5 Å MS (50 mg) in distilled DCM (1.0 mL, 0.1 M) under nitrogen atmosphere at the room temperature. [b] $Sc(OTf)_3$ (0.1 equiv.) and 5 Å MS (50 mg) in distilled DCM (1.0 mL, 0.1 M) under nitrogen atmosphere at the room temperature. MS = molecular sieve; DCM = dichloromethane.

unsaturated *S*-, *N*-, and *C*-glycosides, through glycosylation of the corresponding nucleophiles with **1a**. Of note, in all successful glycosylation instances with heteroatom nucleophiles, there is no direct ring-opening of the DAC moiety. This suggests that intramolecular cyclization may be kinetically favored even in the presence of a heteroatom nucleophile. Following the hard–soft-acid–base (HSAB) principle, oxygen nucleophiles, being hard bases, preferentially add to the hard acid center at C1. Conversely, soft bases like sulfonamide and thiol moieties are inclined to add to the soft acid center at C3.[27] Interestingly, we did not observe any C3-substituted byproducts. Under our conditions, **3s** was produced with high yield and stereoselectivity, though the reaction of **1a** with **2q** and **2r** yielded **3q** and **3r** with moderate yields and imperfect stereoselectivities, respectively. The relatively low yields for **3q** and **3s** were attributed to the unconsumed starting materials in lieu of the C3 attack of the acceptors. It is noteworthy that $Fe(OTf)_3$ was rarely effective in forming C–S bonds. Neither $Cu(OTf)_2$ nor $Fe(OTf)_3$ was effective in creating unsaturated *C*-glycosides when allyltrimethylsilane was used as a nucleophile. Pleasingly, our initial catalyst, $Sc(OTf)_3$, facilitated the formation of allyl *C*-glycosyl derivatives **3t** with good yield (77%) and remarkable stereoselectivity (>30 : 1). Regarding the selectivity preference, according to Danishefsky's work,[28] in our reaction, the preferred stereoselectivity in the construction of *C*-glycosides is not because of the function of the catalyst, but because of the own nature of the allyl nucleophilic reagent. This allylic rearrangement, leveraging ring-strain-release technology, is instrumental in synthesizing the key synthon of 1,6-anhydrosugar **3u** with excellent yield (83%). According to the literature, 1,6-anhydrosugars like **3u** can be transformed into polyfluorinated carbohydrates.[29] These compounds, known for their challenging synthesis and impact on lipophilicity, have garnered significant research interest in recent years as chemical probes or potential therapeutic agents.[30,31] Additionally, 1,6-anhydrosugar **3u** can be used to synthesize biologically relevant polymers found in the cell wall of *Mycobacterium tuberculosis*,[32] and it serves as a suitable intermediate for the total synthesis of bleomycin A2, and heparin-like oligosaccharides,[33] as reported in previous studies.

A series of differentially protected glycals were prepared including conformationally constrained donor CCBz **1b**, galactal donor CCBz **1c**, and L-rhamnal CCBz **1d**. These donors were reacted with three types of acceptors, namely, L-menthol (**Nu^1**) as an aliphatic nucleophile, phenyl 2,3,4-*O*-tri-benzoyl-1-thio-β-glucopyranoside as a sugar nucleophile (**Nu^2**), *para*-methoxylphenol as a phenol nucleophile (**Nu^3**). The results were showed in Table 3. Most cases had good-to-excellent yields and α-selectivities, leading to the formation of 2,3-unsaturated Ferrier-type products. While the 4,6-*O*-constrained glucal **1b** afforded desired products in lower yields of 49%–82% with little change in stereoselectivity (α : β = 9 : 1 to 30 : 1). Like glucal CCBz **1a**, galactal CCBz **1c** could be coupled with **Nu^1**, **Nu^2**, and **Nu^3** to give the desired products in 65%–91% with nearly perfect α-stereocontrollability (α only). The three types

Table 3 Glycal donors scope with different acceptors

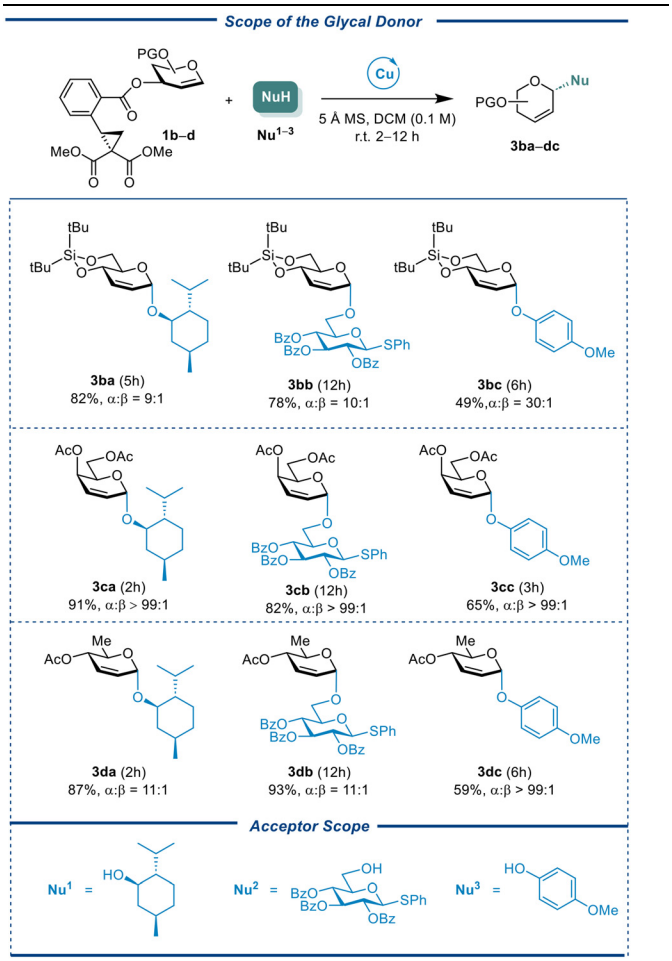

[a] Conditions: unless otherwise noted, all reported yields are isolated and purified products. For Ferrier rearrangement glycosylation reactions of **Nu^1**, **Nu^2**, and **Nu^3**, 1.0 equiv. of the donor **1b–d**, 1.2 equiv. of the acceptor **Nu$^{1–3}$**, and 0.1 equiv. of $Cu(OTf)_2$ was used. r.t. = room temperature; DCM = dichloromethane; Nu = nucleophile; Bz = benzoyl; Ac = acetyl; Ph = phenyl.

of acceptors reacted with the L-rhamnal CCBz **1d** to obtain the required compounds in 59%–93% and mostly α-selectivity (α : β = 11 : 1 to α only). It is worth noting that the aglycon transfer of thioglycoside acceptor was not observed for most glycal CCBz donors, highlighting this method's potential for synthesizing more valuable oligosaccharides.

Finally, galactal donor CCBz **1c** was reacted with **6** (from dapagliflozin which is a drug treating type 2 diabetes) to produce a disaccharide compound **7** with perfect α-selectivity (Scheme 1, a). The rich chemistry of double bonds in this compound supplied a flexible handle for chemical modification to access structurally diverse sodium-glucose cotransporter-2 (SGLT 2) inhibitors.[34] In addition, when deprotected donor **2u** is subjected to $Fe(OTf)_3$-catalyzed conditions, it can undergo synthesis to produce 1,6-anhydrosugar **3u** in high yields on a gram-scale. Likewise, donor **1a** can be effectively treated with diosgenin, a bioactive biomolecule known for its various med-

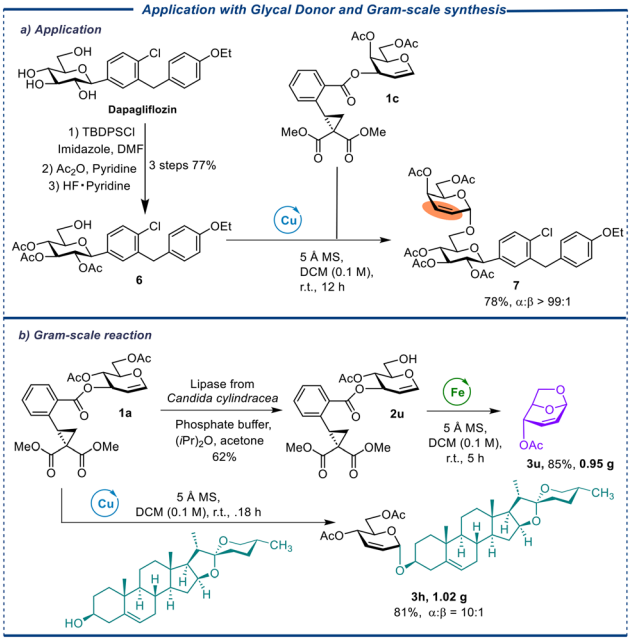

Scheme 1 The application to modifiable dapagliflozin and gram-scale synthesis. Conditions: this reaction was carried out with **1c** (0.1 mmol, 1.0 equiv.), **6** (1.2 equiv.), $Cu(OTf)_2$ (0.1 equiv.); DCM = dichloromethane; DMF = dimethylformamide; Et = ethyl; Ac = acetyl; TBDPS = *tert*-butyldiphenylsilyl.

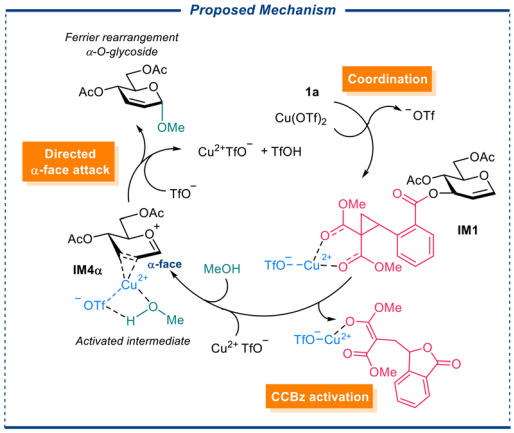

Scheme 2 Proposed stepwise Ferrier rearrangement followed by directed α-face *O*-glycosylation (alcohol attack).

icinal properties such as hypolipidemic, hypoglycaemic, antioxidant, anti-inflammatory, and antiproliferative activities,[35] to synthesize saponin compound **3h** with a high yield and α-selectivity on a gram scale in using $Cu(OTf)_2$ as a catalyst. The successful implementation of gram-scale reactions significantly enhances the competitiveness and appeal of the approach in pharmaceutical synthesis.

To shed light on the stereoselectivity of the glycosylation reaction, we simulated employing model donor **1a** and model acceptors methanol (MeOH), and *p*-methoxyphenol (*p*-OMePhOH) (see ESI†), and $Cu(OTf)_2$, $Sc(OTf)_3$ as the catalysts, we proposed that our $Cu(OTf)_2$-catalyzed Ferrier rearrangement with α-selective glycosylation proceeds in three stages: Firstly, the copper(II)-promoted DAC ring of the CCBz opening resulting in the dissociation of C3-substituent and the migration of the 1,2-double bond, giving rise to an ion pair of the LG anion and glycosyl oxocarbenium. Then another copper(II) species coordinates to the 2,3-position of the glycosyl oxocarbenium **IM4α**, from either α- or β-face, bringing the coordinated alcohol acceptor to the proximity of the glycosyl oxocarbenium. Finally, a directed nucleophilic α-attack by the alcohol at the anomeric position forms the glycosidic bond (Scheme 2). We assumed that the metal center participating in coordination carries an accompanying triflate anion, which serves as a proton acceptor in the final *O*-glycosylation step. Structures of reagents, products, catalysts, proposed intermediates, and transition states were built with GaussView6.0 and pre-optimized at B3LYP/def2-SV(P) level of theory[36] with Grimme's empirical dispersion D3(BJ),[37] and the pre-optimized structures were subjected to geometry optimization and frequency analysis at MN15-L/def2-TZVP/SMD (solvent = DCM) level of theory.[38–40] Accurate electronic energy is calculated from the optimized structures at MN15-L/ma-def2-TZVPP/SMD (solvent = DCM) level of theory.[41] Gibbs free energies of the intermediates were electronic energy calculated as the sum of thermal corrections and the accurate. All calculations were performed with Gaussian 16 software.[42]

Results indicate that in the most stable conformation of the model glucal **1a**, the C3-position CCBz is positioned at the β-face. Coordination of the metal center to the carbonyl groups on CCBz affords **IM1**, with moderate stabilization of the system (ΔG = −5.5 kcal mol^{-1}). Opening of the activated CCBz ring then occurs on **IM1**, and passing through **TS1** ($\Delta G^{\ddagger}_{\mathbf{TS1}}$ = +30.2 kcal mol^{-1}) to give the C3-ring-opened intermediate **IM2**. Inspection of the structure of **IM2** indicated that opening of the strained cyclopropane ring in **IM1** did not directly lead to breakage of the C–O bond, and **IM2** swiftly passes through a following transition state **TS2** ($\Delta G^{\ddagger}_{\mathbf{TS2}}$ = +3.3 kcal mol^{-1}) to give the ion pair constituting the glycosyl oxocarbenium and the dissociated C3-position LG anion **4a**, which remains coordinated to the $Cu(OTf)_2$ and stay close to the glycosyl oxocarbenium at the β-face of the pyranose ring. We have also explored an alternative C3-activation route for CCBz ring opening and dissociation, starting from a stabler intermediate with the $Cu(OTf)_2$ coordinated to both the CCBz carbonyls, C1 and C2 from the β-face, $\mathbf{IM1_{coord}}$, yet the reaction route from this $\mathbf{IM1_{coord}}$ pass through transition states with higher energy barriers, probably due to internal strains (see ESI†), and is hence kinetically disfavored. $Sc(OTf)_3$ the opening and dissociation of the C3-position CCBz following the same route with a similar free energy profile (see ESI†). Upon dissociation of the C3-substituent, the close contacting LG **4a** may linger closely at the β-face of the pyranose ring and block the incoming nucleophiles, resulting in nucleophilic attack from exclusively α-face. Alternatively, if the LG **4a** can freely move away

from the glycosyl oxocarbenium, the calculated NBO charge of the atoms in the oxocarbenium indicated that C1 carries a significant positive charge whilst C2 and C3 do not (NBO charge C1 = +0.37, C2 = −0.38, C3 = +0.02), and a new incoming metal species bringing along with it the alcohol nucleophile (MeOH or *p*-OMePhOH) can presumably coordinate to C2 and C3 on the ring from either α- or β-face after the removal of LG **4a**. DFT simulations of the following nucleophilic addition processes after glucal activation involving MeOH or *p*-OMePhOH acceptors produce similar results leading to the same conclusions, with the α-product from *p*-OMePhOH being more thermodynamically stable than the counterpart from MeOH (ΔG = +0.3 kcal mol^{-1} for β-glucoside from MeOH and +2.6 kcal mol^{-1} for β-glucoside from *p*-OMePhOH), which plausibly contribute to the enhanced α-selectivity of larger acceptors. (Structures from simulation employing MeOH are shown here for discussion, see ESI† for the optimized structures of intermediates and TSs along the reaction routes of *p*-OMePhOH). The optimized structure of **IM4α** and **IM4β** with copper(II) species coordinating from α- or β-face indicated that the metal center can indeed coordinate to C2 and C3 from α-face (Fig. 2c left), but not from β-face. Instead, in the β-face coordination scenario (**IM4β**), the copper(II) center drifts during geometry optimization and preferential coordinates to C3 and carbonyl oxygen at the 4-position of glucal, bringing the acceptor (MeOH or *p*-OMePhOH) away from the anomeric position, and disfavoring directed nucleophilic attack. Importantly, DFT simulations of putative intermediates of a scandium(III) species coordinating to the C=C π-ally system from either face resulted in optimized structures with the metal center dissociated from the C=C system and precluded the formation of stable Sc(OTf)$_3$ coordinated intermediates (see ESI†). Therefore, starting from the only stable copper(II) coordinated intermediate **IM4α** and passing through a tran-

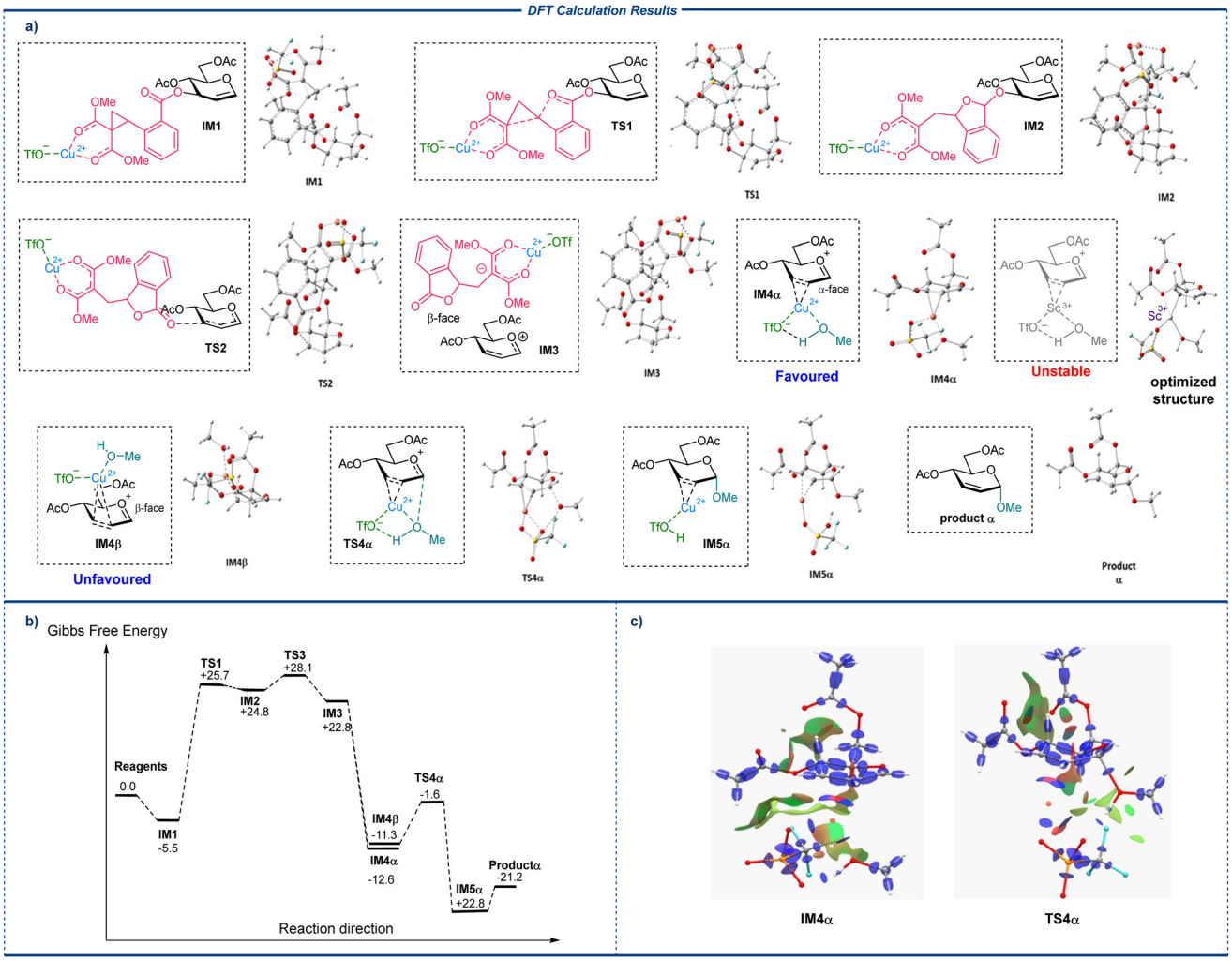

Fig. 2 DFT simulation of the reaction paths. (a) Optimized structures of important intermediates (**IMs**) and transition states (**TSs**) along the main reaction route. (b) The free energy profile along the fastest-rate reaction route from the reagents **1a** and MeOH to the α-glycoside product. The Gibbs free energies are reported in kcal mol^{-1}, with the starting materials taken as reference (0.0). (c) Interaction region indicator (IRI) surfaces of **IM4α** (left) and **TS4α** (right).[43]

sition state of directed nucleophilic attack **TS4α** ($\Delta G^{\ddagger}_{\mathbf{TS4\alpha}}$ = +9.7 kcal mol^{-1}) with moderate energy barrier gives rise to the α-glycosylation product intermediate **IM5**. It is important to note that in **TS4α**, the direction is not directly mediated by the coordination of MeOH to the α-face metal center, but rather the H-bond-like attractive non-covalent interaction between the α-face MeOH and metal bound triflate at the same face (Fig. 2c right). Therefore, DFT results suggest that the preferential α-face metal-triflate mediated direction results in the observed α-stereoselectivity in the glycosylation, which is absent when $Sc(OTf)_3$ with a poorer capability to coordinate to the π-allyl-system. Finally, dissociation of the copper(II) center from **IM5** produces the final α-glycoside.

Conclusion

We have developed a novel Ferrier rearrangement of rationally designed glycal donors with C3-position CCBz, promoted by low-cost and environment-friendly $Cu(OTf)_2$ or $Fe(OTf)_3$ catalysts, enabling efficient synthesis of 2,3-unsaturated glycosides under mild conditions. The new rearrangement approach exhibits high α-stereoselectivity and applies to a wide scope of nucleophile acceptors, affording 2,3-unsaturated *O*-, *S*-, *N*-, and *C*-glycosides with excellent yields. We demonstrate the synthetic potential of our method through the facile construction of a library of natural products of pharmaceutical interest. DFT calculations were performed to elucidate the reaction mechanism, revealing that the high α-stereoselectivity arises from the preferential and directed nucleophilic attack from the α-face mediated by the H-bond interactions between the incoming acceptor and the metal-bound triflate anion, demonstrating the dual role of the catalyst along with the ability of bulky leaving group in directing the stereoselective glycosylation reactions.

Author contributions

X.-W. L. and H. D. conceived the idea. H. Z. established the standard reaction condition. H. Z., H. D., Y. X., Y. Z., and D. Y. conducted the experiments. A. G. performed the DFT calculations. X.-W. L., H. Z., A. G., and H. D. drafted the manuscript. All authors commented on the manuscript. X.-W. L. supervised the whole project.

Data availability

The data supporting this article have been included as part of the ESI.†

Conflicts of interest

There are no conflicts to declare.

Acknowledgements

We thank Nanyang Technological University and the Ministry of Education (MOE-T2EP30120-0007, Tier-1 RG107/23), and the National Research Foundation (NRF-CRP22-2019-0002) from Singapore for the financial support.

References

1 (*a*) N. E. Zachara and G. W. Hart, The Emerging Significance of *O*-GlcNAc in Cellular Regulation, *Chem. Rev.*, 2002, **102**, 431–438; (*b*) R. A. Dwek, Glycobiology: Toward Understanding the Function of Sugars, *Chem. Rev.*, 1996, **96**, 683–720.

2 M. IzuMi, H. Miyazawa, T. Kamakura, I. Yamaguchi, T. Endo and F. Hanaoka, Blasticidin S-resistance Gene (bsr): A Novel Selectable Marker for Mammalian Cells, *Exp. Cell Res.*, 1991, **197**, 229–233.

3 K. Polkowski and A. P. Mazurek, Cytostatic and Cytotoxic Activity of Synthetic Genistein Glycosides Against Human Cancer Cell Lines, *Cancer Lett.*, 2004, **203**, 59–69.

4 J. Popiołkiewicz, K. Polkowski, J. S. Skierski and A. P. Mazurek, In Vitro Toxicity Evaluation in the Development of New Anticancer Drugs—Genistein Glycosides, *Cancer Lett.*, 2005, **229**, 67–75.

5 C. Meier, T. Knispel, E. De Clercq and J. Balzarini, ADA-Bypass by Lipophilic *Cyclo*Sal-ddAMP Pro-nucleotides A Second Example of the Efficiency of the *Cyclo*Sal-Concept, *Bioorg. Med. Chem. Lett.*, 1997, **7**, 1577–1582.

6 S. J. Danishefsky and M. T. Bilodeau, Glycals in Organic Synthesis: the Evolution of Comprehensive Strategies for the Assembly of Oligosaccharides and Glycoconjugates of Biological Consequence, *Angew. Chem., Int. Ed. Engl.*, 1996, **35**, 1380–1419.

7 (*a*) P. Chen and S. Wang, CF_3SO_3H–SiO_2 as Catalyst for Ferrier Rearrangement: An Efficient Procedure for the Synthesis of Pseudoglycosides, *Tetrahedron*, 2013, **69**, 583–588; (*b*) G. Narasimha, B. Srinivas, P. R. Krishna and S. Kashyap, $Zn(OTf)_2$-c atalyzed Glycosylation of Glycals: Synthesis of 2,3-Unsaturated Glycosides via a Ferrier Reaction, *Synlett*, 2014, 523–526; (*c*) P. Chen and S. Li, Y $(OTf)_3$ a s A Highly Efficient Catalyst in Ferrier Rearrangement for the Synthesis of *O*-and *S*-2,3-Unsaturated Glycopyranosides, *Tetrahedron Lett.*, 2014, **55**, 5813–5816; (*d*) P. Chen and S. Wang, Iron(III) triflate, a New Efficient Catalyst for Type I Ferrier Rearrangement, *Tetrahedron*, 2012, **68**, 5356–5262; (*e*) B. G. Williams, S. B. Simelane and H. H. Kinfe, Aluminium Triflate Catalysed *O*-glycosidation: Temperature-switched Selective Ferrier rearrangement or Direct Addition with Alcohols, *Org. Biomol. Chem.*, 2012, **10**, 5636–5642.

8 (*a*) A. M. Gómez, F. Lobo, C. Uriel and J. C. López, Recent Developments in the Ferrier Rearrangement, *Eur. J. Org. Chem.*, 2013, 7221–7262; (*b*) N. Jiang, Z. Wu, Y. Dong, X. Xu, X. Liu and J. Zhang, Progress in the Synthesis of 2,3-

unsaturated Glycosides, *Curr. Org. Chem.*, 2020, **24**, 184–199; (*c*) C. S. Bennett and M. C. Galan, Methods for 2-Deoxyglycoside Synthesis, *Chem. Rev.*, 2018, **118**, 7931–7985; (*d*) A. M. Gómez, F. Lobo, S. Miranda and J. C. López, A Survey of Recent Synthetic Applications of 2,3-Dideoxy-Hex-2-enopyranosides, *Molecules*, 2015, **20**, 8357–8394.

9 M. J. McKay and H. M. Nguyen, Recent Advances in Transition Metal-Catalyzed Glycosylation, *ACS Catal.*, 2012, **2**, 1563–1595.

10 E. B. Bauer, Transition Metal Catalyzed Glycosylation Reactions—an Overview, *Org. Biomol. Chem.*, 2020, **18**, 9160–9180.

11 E. Rafiee, S. Tangestaninejad, M. H. Habibi and V. Mirkhani, A Mild, Efficient and α-Selective Glycosidation by Using Potassium Dodecatungstocobaltate Trihydrate as Catalyst, *Bioorg. Med. Chem. Lett.*, 2004, **14**, 3611–3614.

12 (*a*) K. Toshima, T. Ishizuka, G. Matuo, M. Nakata and M. Kinoshita, Glycosidation of Glycals by 2,3-Dichloro-5,6-dicyano-*p*-benzoquinone (DDQ) as A Catalytic Promoter, *J. Chem. Soc., Chem. Commun.*, 1993, 704–706; (*b*) A. A. Ansari, Y. S. Reddy and Y. D. Vankar, Efficient Carbon-Ferrier Rearrangement on Glycals Mediated by Ceric Ammonium Nitrate: Application to the Synthesis of 2-Deoxy-2-amino-*C*-glycoside, *Beilstein J. Org. Chem.*, 2014, **10**, 300–306.

13 (*a*) N. Bhuma, L. Lebedel, H. Yamashita, Y. Shimizu, Z. Abada, A. Ardá, J. Désiré, B. Michelet, A. Martin-Mingot, A. Abou-Hassan, M. Takumi, J. Marrot, J. Jiménez Barbero, A. Nagaki, Y. Blériot and S. Thibaudeau, Insight into the Ferrier Rearrangement by Combining Flash Chemistry and Superacids, *Angew. Chem., Int. Ed.*, 2021, **60**, 2036–2041, (*Angew. Chem.*, 2021, **133**, 2064–2069); (*b*) M. Takumi, H. Sakaue and A. Nagaki, Flash Electrochemical Approach to Carbocations, *Angew. Chem., Int. Ed.*, 2022, **61**, e202116177, (*Angew. Chem.*, 2022, **134**, e2021161).

14 R. J. Ferrier and G. H. Sankey, Unsaturated Carbohydrates. Part VII. The Preference Shown by Allylic Ester Groupings on Pyranoid Rings for the *Quasi*-axial Orientation, *J. Chem. Soc. C*, 1966, 2345–2349.

15 B. Liberek, D. Tuwalska, A. Konitz and A. Sikorski, X-ray Diffraction and High-resolution NMR Spectroscopy of Methyl 3,4-di-*O*-acetyl-1,5-anhydro-2-deoxy-D-arabino-hex-1-enopyranuronate, *Carbohydr. Res.*, 2007, **342**, 1280–1284.

16 W.-L. Leng, H. Yao, J.-X. He and X.-W. Liu, Venturing Beyond Donor-controlled Glycosylation: New Perspectives Toward Anomeric Selectivity, *Acc. Chem. Res.*, 2018, **51**, 628–639.

17 I. V. Alabugin, L. Kuhn, M. G. Medvedev, N. V. Krivoshchapov, V. A. Vil', I. A. Yaremenko, P. Mehaffy, M. Yarie, A. O. Terent'ev and M. A. Zolfigol, Stereoelectronic Power of Oxygen in Control of Chemical Reactivity: the Anomeric Effect is Not Alone, *Chem. Soc. Rev.*, 2021, **50**, 10253–10345.

18 For our group's recent reports on Ferrier-type glycosylation methodologies, see: (*a*) S. Xiang, Z. Lu, J. He, K. Le Mai Hoang, J. Zeng and X.-W. Liu, β-Type Glycosidic Bond Formation by Palladium-Catalyzed Decarboxylative Allylation, *Chem. Eur. J.*, 2013, **19**, 14047–14051; (*b*) J. Zeng, J. Ma, S. Xiang, S. Cai and X.-W. Liu, Stereoselective β-*C*-Glycosylation by a Palladium-Catalyzed Decarboxylative Allylation: Formal Synthesis of Aspergillide A, *Angew. Chem., Int. Ed.*, 2013, **52**, 5134–5137; (*c*) F. Ding, R. William and X.-W. Liu, Ferrier-Type *N*-Glycosylation: Synthesis of *N*-Glycosides of Enone Sugars, *J. Org. Chem.*, 2013, **78**, 1293–1299; (*d*) S. Xiang, K. Le Mai Hoang, J. He, Y. J. Tan and X.-W. Liu, Reversing the Stereoselectivity of a Palladium-Catalyzed *O*-Glycosylation through an Inner-Sphere or Outer-Sphere Pathway, *Angew. Chem., Int. Ed.*, 2015, **54**, 604–607, (*Angew. Chem.*, 2015, **127**, 614–661); (*e*) L. Ji, S.-H. Xiang, W.-L. Leng, K. Le Mai Hoang and X.-W. Liu, Palladium-Catalyzed Glycosylation: Novel Synthetic Approach to Diverse *N*-Heterocyclic Glycosides, *Org. Lett.*, 2015, **17**, 1357–1360; (*f*) H. Yao, S. Zhang, W.-L. Leng, M.-L. Leow, S. Xiang, J. He, H. Liao, K. Le Mai Hoang and X.-W. Liu, Catalyst-Controlled Stereoselective *O*-Glycosylation: Pd(0) vs Pd(II), *ACS Catal.*, 2017, **7**, 5456–5460; (*g*) N. Huang, H. Liao, H. Yao, T. Xie, S. Zhang, K. Zou and X.-W. Liu, Diastereoselective Synthesis of *C*-Vinyl Glycosides via Gold(I)-Catalyzed Tandem 1,3-Acyloxy Migration/Ferrier Rearrangement, *Org. Lett.*, 2018, **20**, 16–19; (*h*) K. B. Pal, J. Lee, M. Das and X.-W. Liu, Palladium(II)-catalyzed Stereoselective Synthesis of *C*-glycosides from Glycals with Diaryliodonium Salts, *Org. Biomol. Chem.*, 2020, **18**, 2242–2251; (*i*) K. B. Pal, A. Guo, M. Das, J. Lee, G. Báti, B. R. P. Yip, T.-P. Loh and X.-W. Liu, Iridium-promoted Deoxyglycoside Synthesis: Stereoselectivity and Mechanistic Insight, *Chem. Sci.*, 2021, **12**, 2209–2216.

19 H. Ding, J. Lyu, X.-L. Zhang, X. Xiao and X.-W. Liu, Efficient and Versatile Formation of Glycosidic Bonds via Catalytic Strain-release Glycosylation with Glycosyl *Ortho*−2,2-dimethoxycarbonylcyclopropylbenzoate Donors, *Nat. Commun.*, 2023, **14**, 4010.

20 X. Xiao, H. Ding, L.-C. Peng, X.-Y. Fang, Y.-Y. Qin, Q.-Q. Mu and X.-W. Liu, Sweet Strain Release: Donor–Acceptor Cyclopropane Mediated Glycosylation, *CCS Chem.*, 2023, **5**, 2910–2921.

21 V. Pirenne, B. Muriel and J. Waser, Catalytic Enantioselective Ring-Opening Reactions of Cyclopropanes, *Chem. Rev.*, 2021, **121**, 227–263.

22 G. Lian, X. Zhang and B. Yu, Thioglycosides in Carbohydrate Research, *Carbohydr. Res.*, 2015, **403**, 13–22.

23 H. Herzner, T. Reipen, M. Schultz and H. Kunz, Synthesis of Glycopeptides Containing Carbohydrate and Peptide Recognition Motifs, *Chem. Rev.*, 2000, **100**, 4495–4538.

24 R. Sangwan, A. Khanam and P. K. Mandal, An Overview on the Chemical *N*-Functionalization of Sugars and Formation of *N*-Glycosides, *Eur. J. Org. Chem.*, 2020, **2020**, 5949–5977.

25 H. Fukuo, T. Suzuki, J. Shimabukuro, N. Komura, H.-N. Tanaka, A. Imamura, H. Ishida and H. Ando, Synthesis of Diverse Seleno-Glycolipids via the

Transacetalization of Selenoacetals, *Eur. J. Org. Chem.*, 2021, 5455–5467.

26 (*a*) J. Giljanović and A. Prkić, Determination of Coenzyme A (CoASH) in the Presence of Different Thiols by Using Flow-Injection with a UV/Vis Spectrophotometric Detector and Potentiometric Determination of CoASH Using an Iodide ISE, *Molecules*, 2010, **15**, 100–113; (*b*) O. C. M. Sibon and E. Strauss, Coenzyme A: to Make it or Uptake it?, *Nat. Rev. Mol. Cell Biol.*, 2016, **17**, 605–606.

27 (*a*) S. Dharuman, P. Gupta, P. K. Kancharla and Y. D. Vankar, Synthesis of 2-Nitroglycals from Glycals Using the Tetrabutylammonium Nitrate–Trifluoroacetic Anhydride–Triethylamine Reagent System and Base-Catalyzed Ferrier Rearrangement of Acetylated 2-Nitroglycals, *J. Org. Chem.*, 2013, **78**, 8442–8450; (*b*) L. V. Dunkerton, N. K. Adair, J. M. Euske, K. T. Brady and P. D. Robinson, Regioselective Synthesis of Substituted 1-Thiohex-2-enopyranosides, *J. Org. Chem.*, 1988, **53**, 845–850; (*c*) P. Chen, S. Guo, J. Zuo, R. Chu, X. He and G. Zhu, Synthesis of 3-*S*- and 3-*Se*-glycals by Using R-S-S-R and R-Se-Se-R as the Nucleophile Precursors Promoted by $Hf(OTf)_4$ and the Temperature-dependent Formation of the Above-mentioned 3-*S*- and 3-*Se* Products, *Tetrahedron Lett.*, 2020, **61**, 151648.

28 S. Danishefsky and J. F. Kerwin Jr., On the Addition of Allyltrimethylsilane to Glycal Acetates, *J. Org. Chem.*, 1982, **47**, 3803–3805.

29 V. Denavit, D. Lainé, J. St-Gelais, P. A. Johnson and D. Giguère, A Chiron Approach Towards the Stereoselective Synthesis of Polyfluorinated Carbohydrates, *Nat. Commun.*, 2018, **9**, 4721.

30 R. Hevey, The Role of Fluorine in Glycomimetic Drug Design, *Chem. – Eur. J.*, 2021, **27**, 2240–2253.

31 B. Linclau, A. Ardá, N.-C. Reichardt, M. Sollogoub, L. Unione, S. P. Vincent and J. Jiménez-Barbero, Fluorinated Carbohydrates as Chemical Probes for Molecular Recognition Studies. Current Status and Perspectives, *Chem. Soc. Rev.*, 2020, **49**, 3863–3888.

32 L. Wu, Z. Zhou, D. Sathe, J. Zhou, S. Dym, Z. Zhao, J. Wang and J. Niu, Precision Native Polysaccharides from Living Polymerization of Anhydrosugars, *Nat. Chem.*, 2023, **15**, 1276–1284.

33 S.-C. Hung, S. R. Thopate, F.-C. Chi, S.-W. Chang, J.-C. Lee, C.-C. Wang and Y.-S. Wen, 1,6-Anhydro-β-L-hexopyranoses as Potent Synthons in the Synthesis of the Disaccharide Units of Bleomycin A2 and Heparin, *J. Am. Chem. Soc.*, 2001, **123**, 3153–3154.

34 W. Meng, B. A. Ellsworth, A. A. Nirschl, P. J. McCann, M. Patel, R. N. Girotra, G. Wu, P. M. Sher, E. P. Morrison, S. A. Biller, R. Zahler, P. P. Deshpande, A. Pullockaran, D. L. Hagan, N. Morgan, J. R. Taylor, M. T. Obermeier, W. G. Humphreys, A. Khanna, L. Discenza, J. G. Robertson, A. Wang, S. Han, J. R. Wetterau, E. B. Janovitz, O. P. Flint, J. M. Whaley and W. N. Washburn, Discovery of Dapagliflozin: A Potent, Selective Renal Sodium-Dependent Glucose Cotransporter 2 (SGLT2) Inhibitor for the Treatment of Type 2 Diabetes, *J. Med. Chem.*, 2008, **51**, 1145–1114.

35 C. Tohda, T. Urano, M. Umezaki, I. Nemere and T. Kuboyama, Diosgenin is an Exogenous Activator of $1,25D_3$-MARRS/Pdia3/ERp57 and Improves Alzheimer's Disease Pathologies in 5XFAD Mice, *Sci. Rep.*, 2012, **2**, 535.

36 A. D. Becke, Density-Functional Thermochemistry., III. The Role of Exact Exchange, *J. Chem. Phys.*, 1993, **98**, 5648–5652.

37 S. Grimme, S. Ehrlich and L. Goerigk, Effect of The Damping Function in Dispersion Corrected Density Functional Theory, *J. Comput. Chem.*, 2011, **32**, 1456–1465.

38 H. S. Yu, X. He and D. G. Truhlar, MN15-L: A New Local Exchange-Correlation Functional for Kohn–Sham Density Functional Theory with Broad Accuracy for Atoms, Molecules, and Solids, *J. Chem. Theory Comput.*, 2016, **12**, 1280–1293.

39 R. Weigend and F. Ahlrichs, Balanced Basis Sets of Split Valence, Triple Zeta Valence and Quadruple Zeta Valence Quality for H to Rn: Design and Assessment of Accuracy, *Phys. Chem. Chem. Phys.*, 2005, **7**, 3297–3305.

40 A. V. Marenich, C. J. Cramer and D. G. Truhlar, Universal Solvation Model Based on Solute Electron Density and on a Continuum Model of the Solvent Defined by the Bulk Dielectric Constant and Atomic Surface Tensions, *J. Phys. Chem. B*, 2009, **113**, 6378–6396.

41 J. Zheng, X. Xu and D. G. Truhlar, Minimally Augmented Karlsruhe Basis Sets, *Theor. Chem. Acc.*, 2011, **128**, 295–305.

42 M. J. Frisch, G. W. Trucks, H. B. Schlegel, G. E. Scuseria, M. A. Robb, J. R. Cheeseman, G. Scalmani, V. Barone, G. A. Petersson, H. Nakatsuji, X. Li, M. Caricato, A. V. Marenich, J. Bloino, B. G. Janesko, R. Gomperts, B. Mennucci, H. P. Hratchian, J. V. Ortiz, A. F. Izmaylov, J. L. Sonnenberg, D. Williams-Young, F. Ding, F. Lipparini, F. Egidi, J. Goings, B. Peng, A. Petrone, T. Henderson, D. Ranasinghe, V. G. Zakrzewski, J. Gao, N. Rega, G. Zheng, W. Liang, M. Hada, M. Ehara, K. Toyota, R. Fukuda, J. Hasegawa, M. Ishida, T. Nakajima, Y. Honda, O. Kitao, H. Nakai, T. Vreven, K. Throssell, J. A. Montgomery Jr., J. E. Peralta, F. Ogliaro, M. J. Bearpark, J. J. Heyd, E. N. Brothers, K. N. Kudin, V. N. Staroverov, T. A. Keith, R. Kobayashi, J. Normand, K. Raghavachari, A. P. Rendell, J. C. Burant, S. S. Iyengar, J. Tomasi, M. Cossi, J. M. Millam, M. Klene, C. Adamo, R. Cammi, J. W. Ochterski, R. L. Martin, K. Morokuma, O. Farkas, J. B. Foresman and D. J. Fox, *Gaussian 16, Revision C.01*, Gaussian, Inc., Wallingford, CT, 2016.

43 T. Lu and Q. Chen, Interaction Region Indicator: A Simple Real Space Function Clearly Revealing Both Chemical Bonds and Weak Interactions, *Chem.: Methods*, 2021, **1**, 231–239.

